URSI-RCRS 2024, Aries/GEHU, Bhimtal, India, 22 – 25 October, 2024

Unveiling Low-Frequency Eclipses in Spider MSPs with GMRT Observations

Sangita Kumari[1], Bhaswati Bhattacharyya*[1]
(1) National Centre for Radio Astrophysics, Pune, India

Abstract

Low-frequency eclipse studies have been reported for only $\sim$ 8% of spider millisecond pulsars (MSPs). These studies are crucial for probing the properties of the eclipse medium, as eclipses are more prominent at lower frequencies. In this study, we increase the sample by $\sim$ 13% and present interesting results for individual sources. We aim to enhance the understanding of eclipsing phenomena in MSPs by investigating low-frequency eclipses using wide-bandwidth observations from the Giant Metrewave Radio Telescope (GMRT). We report the first evidence of eclipsing for PSR J2234+0944 and PSR J2214+3000 in one observation epoch, with no eclipsing observed in subsequent epochs, indicating temporal evolution of the cutoff frequency in these systems. For PSR J1555–2908 and PSR J1810+1744, we established constraints on the eclipse cutoff frequency, estimating it to be above 740 MHz. Additionally, we calculated the mass loss rates of the companions for PSR J1555–2908 and PSR J1810+1744, finding these rates insufficient to ablate the companion stars. For the first time, we detected an eclipse at a non-standard orbital phase for PSR J1810+1744. This eclipse, observed during the second orbit but not the first, indicates significant dynamic changes within the system. Our study also reveals that a higher spin-down flux of the pulsar at the companion's location does not necessarily lead to eclipses, highlighting the complex interactions within these systems. These findings contribute to the broader goal of understanding the dynamics and environmental conditions that govern eclipsing behavior in MSP systems.

1 Introduction

Eclipsing spider MSPs are compact binaries in which the energetic pulsar wind ablates the companion and this ablated material is assumed to be the cause of observed eclipses (e.g. $\sim$ 10% of the binary orbit is eclipsed for PSR J1959+2048, 1). Based on the mass of the companion (M_c), spider MSPs are divided into two categories: black widow (BW, $M_c < 0.05M_\odot$, 2) and redback (RB, $0.1M\odot < M_c < 0.9M_\odot$, 2). Owing to the frequency-dependent nature of the eclipses, the pulsed signal from the pulsar disappears within the eclipse region below a certain frequency called the eclipse cut−off frequency (ν_c).

With the advent of new telescopes, the population of spider MSPs is steadily increasing, yet eclipses are observed in very few of these systems. For example, PSRs J0023+0924, J2214+3000, and J2234+0944 (3) are a few systems where no signature of radio eclipses has been seen. The scarcity of eclipses could stem from the lack of low-frequency observations, as eclipses are more prominently detected at lower frequencies. A second reason for the non-detection of eclipses could be the low orbital inclination angle, which prevents the pulsar's radio waves from passing through the ablated material of the companion. A third potential reason for the non-detection of eclipses could be that the companion star fails to fill its Roche lobe. Discovering and studying more spider systems exhibiting eclipses is of prime importance. Spider MSPs are thought to be the progenitors of isolated MSPs. Thus far, no spider MSP system has been identified in which it is feasible to completely ablate the companion within a reasonable timescale. For instance, for PSR J2051–0827, the mass loss rate ($\dot{m}_c$) is $10^{-14}M_\odot$/year (4); for PSR J1959+2048 and PSR J1816+4510, $\dot{m}_c$ is 10^{-12} and $2 \times 10^{-13}M_\odot$/year (5), respectively; and for PSR J1544+4937, $\dot{m}_c$ is $1.9 \times 10^{14}M_\odot$/year (6). Hence, finding eclipses using low-frequency observations in more spider systems would allow us to calculate the mass loss rate, contributing to the search for such a pulsar. With the advent of wide-bandwidth radio telescopes, precise estimation of eclipse cutoff frequencies has become possible, as demonstrated by (7) for PSR J1544+4937 using the upgraded GMRT. Determining the cutoff frequencies for other spider systems would enable the study of the probable eclipse mechanisms. Previous study by (8) suggested various mechanisms to explain the low-frequency eclipses in these systems. For example, cyclotron-synchrotron absorption is believed to be the major eclipse mechanism for PSR J1810+1744 (9), and J1227–4853 (10), while scattering and cyclotron absorption are considered the primary mechanisms for PSR J2051–0827 (11). Furthermore, stimulated Raman scattering has been suggested as the most plausible eclipse mechanism for PSR B1744–24A (8). Observing temporal variations in the eclipse cutoff frequencies would also allow us to study the dynamic changes occurring in the eclipse environment, including changes in electron column density and magnetic field (6). The frequency-dependent nature of the eclipses makes them easier to detect at lower frequencies compared to higher frequencies. Therefore, the upgraded GMRT (uGMRT) is the perfect instrument for studying frequency-dependent eclipsing, as it allows for wide-bandwidth observations at low frequencies ($\sim$ 300 MHz). Additionally, the wide bandwidth provided by uGMRT enables precise estimation of the eclipse cutoff frequency.

Table 1. Table listing the cut−off frequency values for multiple observing epochs along with corresponding electron column density.

Pulsar name	Date	Cutoff frequency(ν_c)	$N_e^a(cm^{-2})$	$R_E^b(cm)$	M_c^c ($M_\odot/year$)
J1555−2908	29-06-2020	> 740	7×10^{16}	-	-
	04-07-2020	> 740	11×10^{16}	6.6×10^{10}	6.5×10^{-13}
J1810+1744	26-06-2020$_1$	> 740	$7\times10^{16*}$	1.5×10^{11}	8.7×10^{-13}
	26-06-2020$_2$	> 740	$4\times10^{16*}$	1.5×10^{11}	6.5×10^{-13}

[a]: The maximum electron density in the eclipse medium; [b]: Eclipse radius; [c]: Mass loss rate of the companion; [*]: The epochs where only the limit on the N_e is known; [1]: 1st orbit; [2]: 2nd orbit.

2 Results

In this paper we are reporting the low frequency study for a sample 4 spider MSPs, namely J2214+3000, J2234+0944, J1555–2908 and J1810+1744. The observations were conducted in band 3 (300–500 MHz), band 4 (550–750 MHz), and band 5 (1050–1450 MHz) of the uGMRT. In the following sections, the results from this study are presented.

2.1 First evidence of eclipsing for PSR J2214+3000 & PSR J2234+0944

We analyzed band 3 and band 4 data near the eclipse phase (orbital phase $\sim$ 0.2–0.3) over three epochs to investigate eclipsing in PSR J2214+3000 and PSR J2234+0944. Figure 1 shows the detection plots for both pulsars on 11 November 2022. Previous low-frequency study by (3), which covered frequencies from 385 MHz to 1.5 GHz using various radio telescopes (WSRT, Effelsberg, Lovell, Nancy Radio Telescope), did not report eclipses for these pulsars. They also studied orbital phase-dependent DM variations and found no DM increase near the superior conjunction (orbital phase 0.25), indicating the absence of eclipsing material. However, they suggested that this might be due to coarse DM sampling over the orbital period. For the first time, we detected frequency-dependent eclipsing in PSR J2214+3000 and PSR J2234+0944 on 11 November 2022. As shown in Figure 1a, PSR J2214+3000 was not detected during the eclipse phase (0.23 to 0.26) in Band 3, but only showed flux fading in Band 4. Similarly, Figure 1b shows that PSR J2234+0944 was not detected in Band 3 during the eclipse phase, but was detected in Band 4. No eclipsing signatures were noted in other epochs for either pulsar. This indicates that the eclipse environment for these systems is dynamically evolving, as seen in other BW MSP systems, such as PSR J1544+4937 (6). As part of the European Pulsar Timing Array (EPTA), detecting eclipses in these systems may have implications for EPTA, as the eclipse phase should be neglected while searching for gravitational wave signals.

2.2 Determination of eclipse cutoff frequency for PSR J1555−2908, PSR J1810+1744

We analyzed the band 4 and band 5 observation data for PSR J1810+1744 with the aim to find the eclipse cutoff frequency. In the previous studies eclipse has been reported upto 750 MHz by (9) for this pulsar. Figure 2 shows the detection plots for two consecutive eclipses on 26 June 2020. The pulsar is detected in band 4, where a complete eclipse is observed in both epochs. However, the pulsar is not detected in simultaneous band 5 observations. This depicts that the eclipse cutoff frequency for this system is above band 4 of uGMRT. For PSR J1555−2908, (12) found eclipses at 820 MHz for 10% of the orbit using the Green Bank Telescope (GUPPI pulsar backend with 200 MHz bandwidth). Therefore we observed this MSP in band 3, band 4 and band 5 of uGMRT with the aim to find the eclipse cutoff frequency, as it would either be in band 5 or would be above that. The pulsar is detected at band 4 and band 3 as evident from Figure 3, however the pulsar is not detected at band 5, which could be due to its inverted spectra. We could not detect a precise value of the eclipse cutoff frequency for this system as we found complete eclipsing in band 3 and band 4 and conclude that it would be above band 4. We also observed the flux density decrease near the eclipse boundary along with the rise in the DM near the

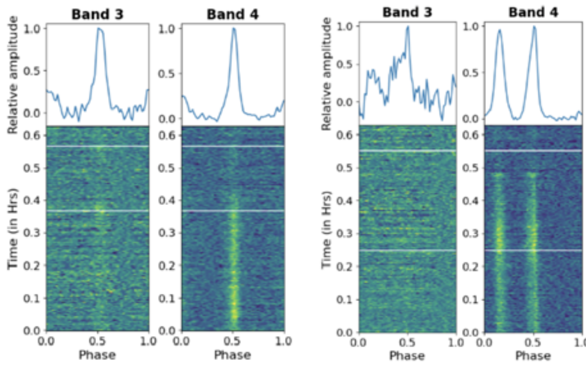

(a) PSR J2214+3000 (b) PSR J2234+0944

Figure 1. Phase versus time plot showing the first evidence of eclipsing for PSR J2214+3000 and PSR J2234+0944 for simultaneous band 3 and band 4 observations on 11 November 2022. a) The white lines covers the orbital phase from 0.23−0.26. The eclipse can be seen in band 3, and flux fading can be observed in band 4. b) The white lines covers the orbital phase from 0.25−0.28. Eclipse is observed in band 3; however, no eclipse is noted in band 4.

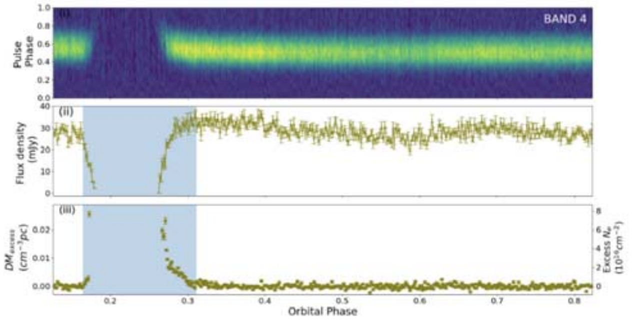

(a) First eclipse for J1810+1744

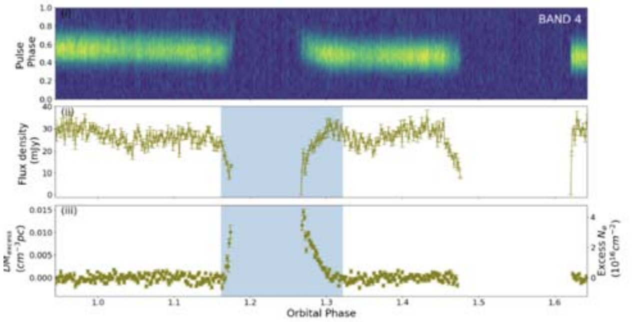

(b) Second eclipse for J1810+1744

Figure 2. The consecutive eclipses for PSR J1810+1744 on 26 June 2020. Three panels, from top to bottom depict variation of (i) the total intensity at band 4 (ii) flux density of total intensity at band 4(iii) excess DM (DM_{excess}) along the line of sight at band 4.

eclipse boundary as can be noted from Figure 3, as seen for other BW MSPs. The corresponding value of N_e is given in Table 1.

2.3 First detection of eclipse at non standard orbital phase for PSR J1810+1744

For the second eclipse covered for PSR J1810+1744, the presence of an eclipse at a non-standard orbital phase (orbital phase $\sim$ 0.55) is seen, along with the main eclipse around the superior conjunction (orbital phase $\sim$0.25). Figure 2b depicts the orbital phase DM and flux density plot for the second eclipse observed. This is very strange, as the presence of another eclipse at an orbital phase of approximately 0.5 cannot be seen for the first orbit covered but is suddenly noted for the next orbit. This suggests that the system is very dynamic, with extra material suddenly appearing at the orbital phase of 0.5. It can also be noted that the length of the eclipse at the 0.55 orbital phase is longer than at the 0.25 orbital phase. Eclipses other than at superior conjunction have also been observed for other BW MSPs in the past. For example, a mini eclipse has been reported for PSR J1544+4937 by (13). The cause of the mini eclipse could be the anisotropic and clumpy distribution of ionized gas in the orbit.

2.4 Mass loss rate estimation

We estimated the mass loss rates of the companions for PSR J1810+1744 and PSR J1555–2908 in our sample, for which we report eclipses at band 4 of the uGMRT. The estimated mass loss rates are provided for both pulsars in Table 1. For PSR J1555–2908, the mass loss rate on 04 July 2020 is 6.5×10^{-13} $M_{\odot}/year$. However, we could not determine the mass loss rate on 29 June 2020 for this pulsar, as the complete eclipse was not covered. For PSR J1810+1744, we estimated the mass loss rates to be 8.7×10^{-13} $M_{\odot}/year$ and 6.5×10^{-13} $M_{\odot}/year$ for the first and second eclipses observed on 26 June 2020, respectively. The estimated mass loss rates for both pulsars are not sufficient to evaporate the companion within the Hubble timescale.

2.5 Eclipse width as the function of frequency for PSR J1810+1744

We investigated how the eclipse width varies as a function of frequency by dividing the 200 MHz wide bandwidth uGMRT data into smaller chunks ($\sim$ 28 MHz). This analysis was conducted for the consecutive main eclipses observed in our dataset ($\sim$ 0.25) and the eclipse occurring at a non-standard orbital phase ($\sim$ 0.5). Our study did not reveal any significant frequency evolution of the eclipse width, either for the main eclipse or for the eclipse at the non-standard orbital phase ($\sim$ 0.5). The eclipse width appears to be nearly constant with frequency or may vary very slowly within the observed band, with changes smaller than the length of a sub-integration in time. Assuming that the scaling of the eclipse width (E_w) with frequency is $E_w = K\nu^{-\alpha}$, and given that the eclipse width could not change more than the length of a sub-integration, we constrained the value of α to be less than 0.22. Several eclipse mechanism are proposed by (8) to explain the frequency-dependent eclipsing observed in spider MSPs. Each mechanism results in a different evolution of eclipse width with frequency (i.e., different values of α). Therefore, by determining the value of α, the eclipse mechanism in PSR J1810+1744 can be probed.

2.6 The $Edot/a^2$ correlation

The mass loss of the binary companion can be due to the three primary reason. First, the evaporative mass loss, due to heating effects by the pulsar energetic wind and γ-ray emission from the intra-binary shock region. Due to the heating of the companion, it may gets bloated and fill its Roche lobe, and Roche lobe overflow could be the second cause of the mass loss. Thirdly, the pulsar energetic winds can directly ablate the mass off the companion. From the ATNF pulsar catalogue, we inferred the $\dot{E}/a^2$, value for spider MSPs population. $\dot{E}/a^2$ is measure of how much the pulsar wind and energetic radiation would be effective at the position of the companion. $\dot{E}/a^2$ value was available for a sample of 33 eclipsing spider MSP and for a sample of 21 non-eclipsing spider MSPs. We found the $\dot{E}/a^2$ of the same order for spider MSP population showing eclipse and spider MSP population not showing eclipse. Moreover, we also found that there are few non-eclipsing spider systems (for example PSR J0024$-$7204P and J0024$-$7204R), for which the $\dot{E}/a^2$ value is $\sim 2 \times 10^{35}$ erg/s ${R_{\odot}}^2$, yet they do not show any signature of the eclipse. This indicates that the other factors such as the orbital inclination angle plays a significant role for the presence of eclipse.

3 Summary

This paper presents the initial detection of eclipsing events in PSR J2214+3000 and PSR J2234+0944 during a single observational epoch. Subsequent observations over two epochs did not reveal further eclipsing, suggesting a dynamic evolution of the eclipse environment in these systems. Additionally, we identified that the eclipse cutoff frequency for PSRs J1555−2908 and J1810+1744 exceeds Band 4. Notably, alongside the primary eclipse, we observed, for the first time, an eclipse occurring at a non-standard orbital phase for PSR J1810+1744, which has not been previously reported. The cause of this occurrence requires further investigation. Furthermore, our study of eclipse width as a function of frequency for PSR J1810+1744 did not indicate any variation. Based on these findings, we derived constraints on the parameter α, influencing the potential eclipse mechanism. Moreover, our results highlight that a higher spin-down flux of the pulsar at the companion's location does not invariably guarantee the presence of eclipses in these systems. These insights deepen our understanding of pulsar eclipses, revealing complexities in their occurrence.

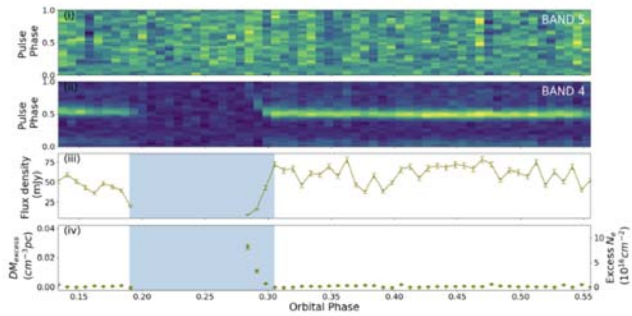

(a) 04 July 2019 plots for PSR J1555−2908

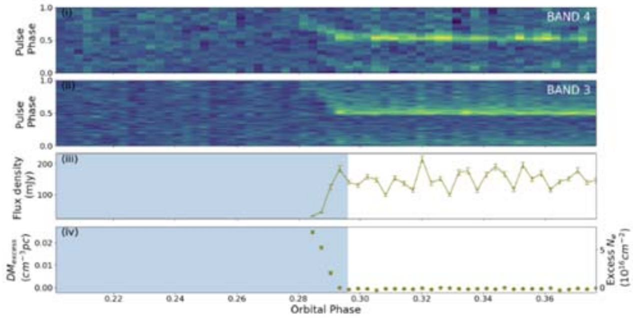

(b) 29 June 2019 plots for PSR J1555−2908

Figure 3. Detection plots for PSR J1555−2908 for two different epochs. a) Four panels, from top to bottom depict variation for 4 July 2019 of (i) the total intensity at band 5, (ii) the total intensity at band 4, (iii) flux density of total intensity at band 4, (iv) excess DM (DM_{excess}) along the line of sight. b) Four panels, from top to bottom depict variation for 29 July 2019 of (i) the total intensity at band 4, (ii) the total intensity at band 3, (iii) flux density of total intensity at band 3, (iv) excess DM (DM_{excess}) along the line of sight.

References

[1] Fruchter, A. S., Stinebring, D. R., & Taylor, J. H. 1988, Nature, 333, 237

[2] Roberts, M. S. 2012, Proceedings of the International Astronomical Union, 8, 127

[3] Bak Nielsen, A.-S., Janssen, G. H., Shaifullah, G., et al. 2020, Monthly Notices of the Royal Astronomical Society, 494, 2591

[4] Stappers, B., Bailes, M., Lyne, A., et al. 1996, The Astrophysical Journal, 465, L119

[5] Polzin, E., Breton, R., Bhattacharyya, B., et al. 2020, Monthly Notices of the Royal Astronomical Society, 494, 2948

[6] Kumari, S., Bhattacharyya, B., Sharan, R., et al. 2024, ApJ, 961, 155

[7] Kansabanik, D., Bhattacharyya, B., Roy, J., & Stappers, B. 2021, The Astrophysical Journal, 920, 58

[8] Thompson, C., Blandford, R. D., Evans, C. R., & Phinney, E. S. 1994, ApJ, 422, 304

[9] Polzin, E. J., Breton, R. P., Clarke, A. O., et al. 2018, MNRAS, 476, 1968

[10] Kudale, S., Roy, J., Bhattacharyya, B., Stappers, B., & Chengalur, J. 2020, ApJ, 900, 194

[11] Polzin, E. J., Breton, R. P., Stappers, B. W., et al. 2019, MNRAS, 490, 889

[12] Ray, P. S., Nieder, L., Clark, C. J., et al. 2022, ApJ, 927, 216

[13] Bhattacharyya, B., Roy, J., Ray, P., et al. 2013, The Astrophysical journal letters, 773, L12